

1 Supplemental Information for

2 **Secondary organic aerosol formation and primary organic aerosol oxidation**
3 **from biomass burning smoke in a flow reactor during FLAME-3**

4 A. M. Ortega^{1,2}, D. A. Day^{1,3}, M. J. Cubison^{1,3*}, W. H. Brune⁴, D. Bon^{1,3,5**}, J. de Gouw^{1,5}, and J. L. Jimenez^{1,3}

5 ¹Cooperative Institute for Research in the Environmental Sciences, Boulder, CO, USA

6 ²Department of Atmospheric and Oceanic Sciences, University of Colorado, Boulder, CO, USA

7 ³Department of Chemistry and Biochemistry, University of Colorado, Boulder, CO, USA

8 ⁴Department of Meteorology, Pennsylvania State University, University Park, PA, USA

9 ⁵Chemical Sciences Division, NOAA Earth System Research Laboratory, Boulder, CO, USA

10 * now at: Tofwerk AG, Thun, Switzerland

11 ** now at: Planning and Policy Program, Air Pollution Control Division, Colorado Department of Public Health and
12 Environment, Denver, CO

13

14 **Discussion of Figure S3.**

15 The standard AMS fragmentation table is the foundation for calculating OA mass in ambient
16 AMS measurements (Allan et al., 2004). Unlike typical ambient observations, OA dominated
17 the total aerosol mass spectra (campaign averaged, OA was 93% of total aerosol). Hence, the
18 standard fragmentation table needed to be adjusted to account for high organic-mass loadings
19 (see Fig. S3). In this modification, sulfate was treated as interference on the organic peaks, as
20 opposed to organic as an interference on the sulfate peaks, as in the default treatment of the
21 “ambient” fragmentation table. To accomplish this, m/z 48 was used as the basis for estimating
22 the sulfate contribution. As seen in Fig. S3, the ratio of dominant ions at m/z 48, C_4^+ and SO^+ ,
23 were plotted as a function of OA mass to show that this ratio asymptotes to a constant value with
24 increasing OA mass. See Table S1 for the modified fragmentation table.

25 **Figure Captions:**

26 **Table S1.** Standard AMS fragmentation table for unit mass resolution (UMR) analysis and
27 updated table for calculating sulfate and organic mass fragments for biomass burning smoke
28 measurements with high organic fraction of total aerosol mass.

29 **Fig. S1:** Photo of (a) Fire Sciences Laboratory's (FSL) fire chamber in open/chamber burn
30 configuration for burn 58, saw grass, taken by Dan Bon, (b) PAM reactor in open-flow-through
31 configuration with both lamps on, taken by Amber Ortega.

32 **Fig. S2:** Sawtooth pattern from switching OA measurements (light lines) between aged (dashed
33 lines) and unprocessed (solid lines) sampling for organic aerosol and aerosol markers: oxidation
34 (m/z 44, pink lines) and primary biomass burning (m/z 60, brown lines) for two burns, turkey oak
35 (burn 45) and ponderosa pine (burn 40). Tags indicate typical operations, such as changes in OH,
36 filters, and sampling.

37 **Fig. S3.** A procedure developed to correctly calculate sulfate and organic concentrations for
38 biomass burning smoke. The top left plot is the ratio of C_4^+ to SO^+ at m/z 48 vs. unprocessed OA
39 mass, colored by SO^+ ion signal for three fuels (ponderosa pine, burn 40; lodgepole pine burn 50;
40 and turkey oak, burn 45). The rest of the plots compare standard fragmentation table calculations
41 of sulfate to the updated biomass burning specific UMR fragmentations table (see Table S1) for
42 burn 42, wire grass. The top right plot is a time series of sulfate from standard (labeled "Std Frag
43 SQ") and updated (labeled "BB Frag SQ") calculations for UMR (red) and high-resolution
44 (black) data. The bottom left plot is the mass spectra of sulfate from standard (labeled "Std Frag
45 SQ") and updated (labeled "BB Frag SQ") calculations, and the bottom right plot is the sulfate
46 mass spectra comparison of UMR (labeled "SQ") and high-resolution (labeled "PK") data for the
47 standard (labeled "Std Frag SQ") and updated (labeled "BB Frag SQ").

48 **Fig. S4.** (a) Comparison of organic mass time series for all data from all burns of unit mass
49 resolution to high-resolution analysis (as calculated up to m/z 100). (b) Cation balance with high-
50 resolution data, measured to predicted cations K^+ and NH_4^+ based on neutral inorganic ion
51 stoichiometry.

52 **Fig. S5.** Average difference (open-closed) high-resolution spectrum at m/z 28 averaged from
53 08:46:00–08:57:00 on 9/22/2009 during burn 42, wire grass for (a) aged and (b) unprocessed
54 smoke. Note that the contribution of CO^+ from $CO(g)$ is negligible due to the strong
55 discrimination against gases (by 10^7) by the AMS inlet.

56 **Fig. S6.** OH_{exp} as calculated from offline SO_2 calibrations versus OH_{exp} calculated from real-time
57 VOC decays with all data in light circles and stable data in dark circles for benzene (red) and
58 toluene (blue).

59 **Fig. S7.** Evolution of aerosol ions at m/z 28 and m/z 44 from high-resolution analysis for two
60 biomass fuels, turkey oak (burn 45) and ponderosa pine (burn 40), normalized to peak CO^+ and
61 CO_2^+ concentration in each burn. The saw-tooth pattern is the result of switching between aged
62 and the unprocessed smoke sample.

63 **Fig. S8.** The mass spectra ratio, ER_{OA} , of aged to unprocessed smoke of two fuels: turkey oak,
64 burn 45, and ponderosa pine, burn 40, where an increase in ion signal is shown in green ($ER_{OA} >$
65 1) and decrease in ion signal ($ER_{OA} < 1$) is shown in red.

66 **Fig. S9.** Fractional contribution of oxidation and biomass burning tracers vs. POA concentration.
67 (a) f_{44} vs. POA for unprocessed smoke from all burn experiments. (b) f_{60} vs. POA for
68 unprocessed smoke from all burn experiments. (c) Aging effects on $f_{CO_2^+}$ and biomass-burning
69 marker, f_{60} , for four select fuels (ponderosa pine, burn 40; wire grass, burn 42; turkey oak, burn
70 45; and sage, burn 49). Dotted lines are from ambient biomass burning measurements from
71 Cubison et al. (2011).

72 **Fig. S10.** Van Krevelen diagram, showing hydrogen-to-carbon (H/C) ratio vs. oxygen-to-carbon
73 ratio (O/C). (a) Six fuels (ponderosa pine, burn 40; pocosin, burn 41; wire grass, burn 42; turkey
74 oak, burn 45; sage, burn 49; and lodgepole pine, burn 61), with associated slopes from a linear
75 orthogonal distance regression fit. (b) All fuels, with associated slopes from a linear orthogonal
76 distance regression fit reported in legend (lines not shown for simplicity), slopes from Heald et
77 al. (2010; solid lines), ambient measurements of OOA data first presented in f_{44}/f_{43} space in Ng
78 et al. (2010) and transformed in to Van Krevelen space in Ng et al. (2011)'s work (dashed lines)
79 with shaded region (gray area) denoting $\pm 10\%$ uncertainty.

Table S1.**Standard Frag Table for Unit Mass Resolution AMS Analysis**

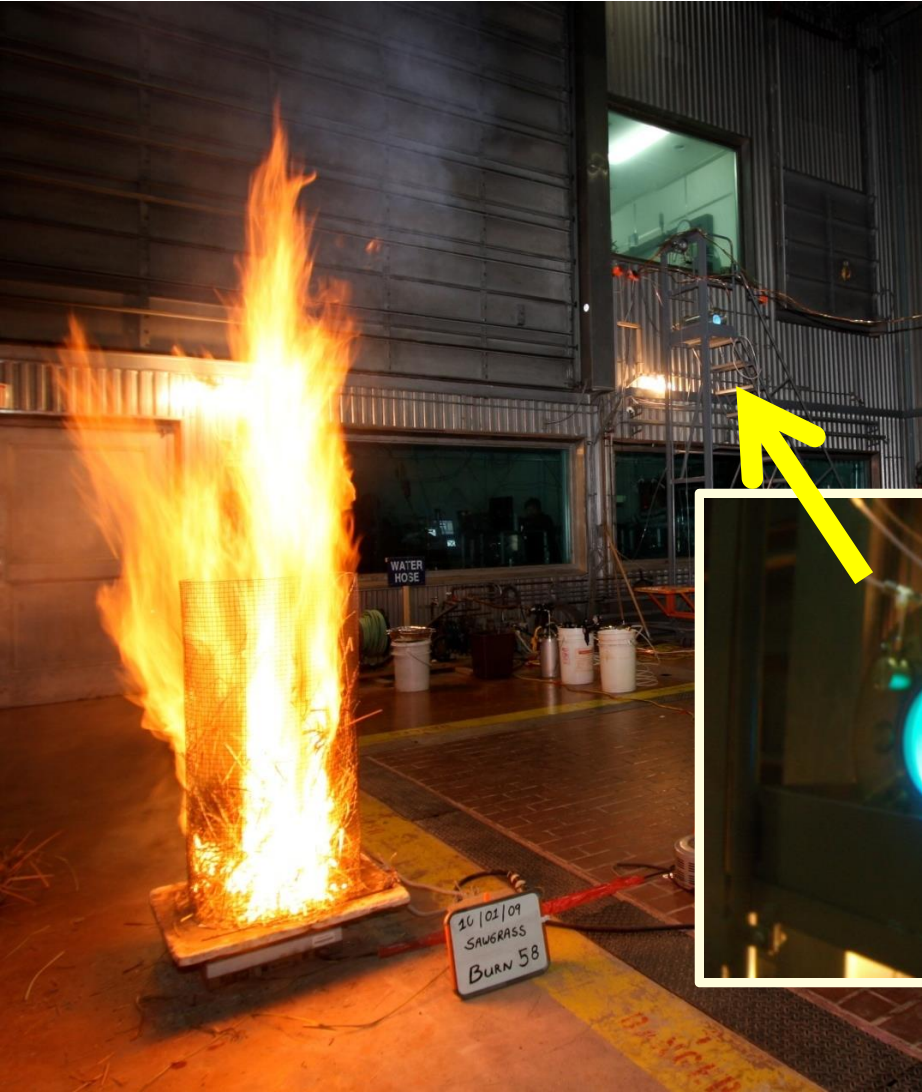
<i>m/z</i>	<i>frag_organic</i>	<i>frag_sulphate</i>	<i>frag_SO3</i>	<i>frag_H2SO4</i>
48	0.5*frag_organic[62]	frag_SO3[48], frag_H2SO4[48]	48,-frag_organic[48],-frag_nitrate[48], -frag_H2SO4[48]	.5*.93*frag_H2SO4[81], .5*.93*frag_H2SO4[98]
64	0.5*frag_organic[50],0.5*frag_organic[78]	frag_SO3[64], frag_H2SO4[64]	64,-frag_organic[64],-frag_H2SO4[64]	0.5*0.93*frag_H2SO4[81], 0.5*0.93*frag_H2SO4[98]
80	0.75*frag_organic[94]	frag_SO3[80], frag_H2SO4[80]	0.25*80,-0.25*frag_organic[80]	0.75*80,-0.75*frag_organic[80]
81	0.5*frag_organic[67],0.5*frag_organic[95]	frag_H2SO4[81]		81,-frag_organic[81]
98	0.5*frag_organic[84],0.5*frag_organic[112]	frag_H2SO4[98]		98,-frag_organic[98]

Updated Frag Table for Unit Mass Resolution AMS Analysis

<i>m/z</i>	<i>frag_organic_BB</i>	<i>frag_sulphate_BB</i>
48	0.032*0.5*frag_organic_BB[47], 0.032*0.5*frag_organic_BB[49]	48,-frag_organic_BB[48]
64	64,-frag_sulphate_BB[64]	1.14*frag_sulphate_BB[48]
80	80,-frag_sulphate_BB[80]	0.32*frag_sulphate_BB[48]
81	81,-frag_sulphate_BB[81]	0.23*frag_sulphate_BB[48]
98	98,-frag_sulphate_BB[98]	0.124*frag_sulphate_BB[48]

Figure S1.

(a)



(b)

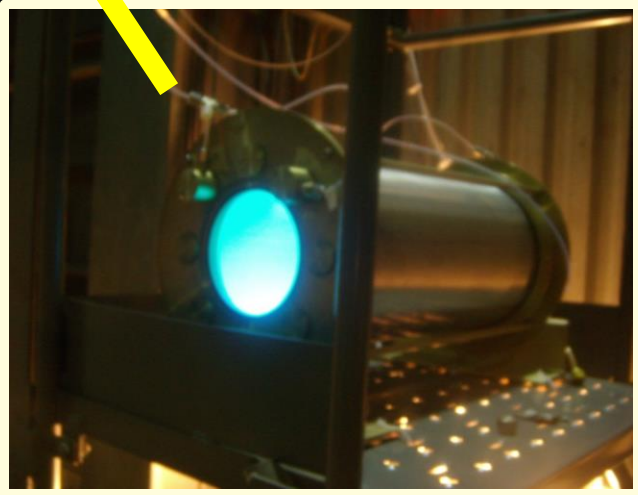


Figure S2.

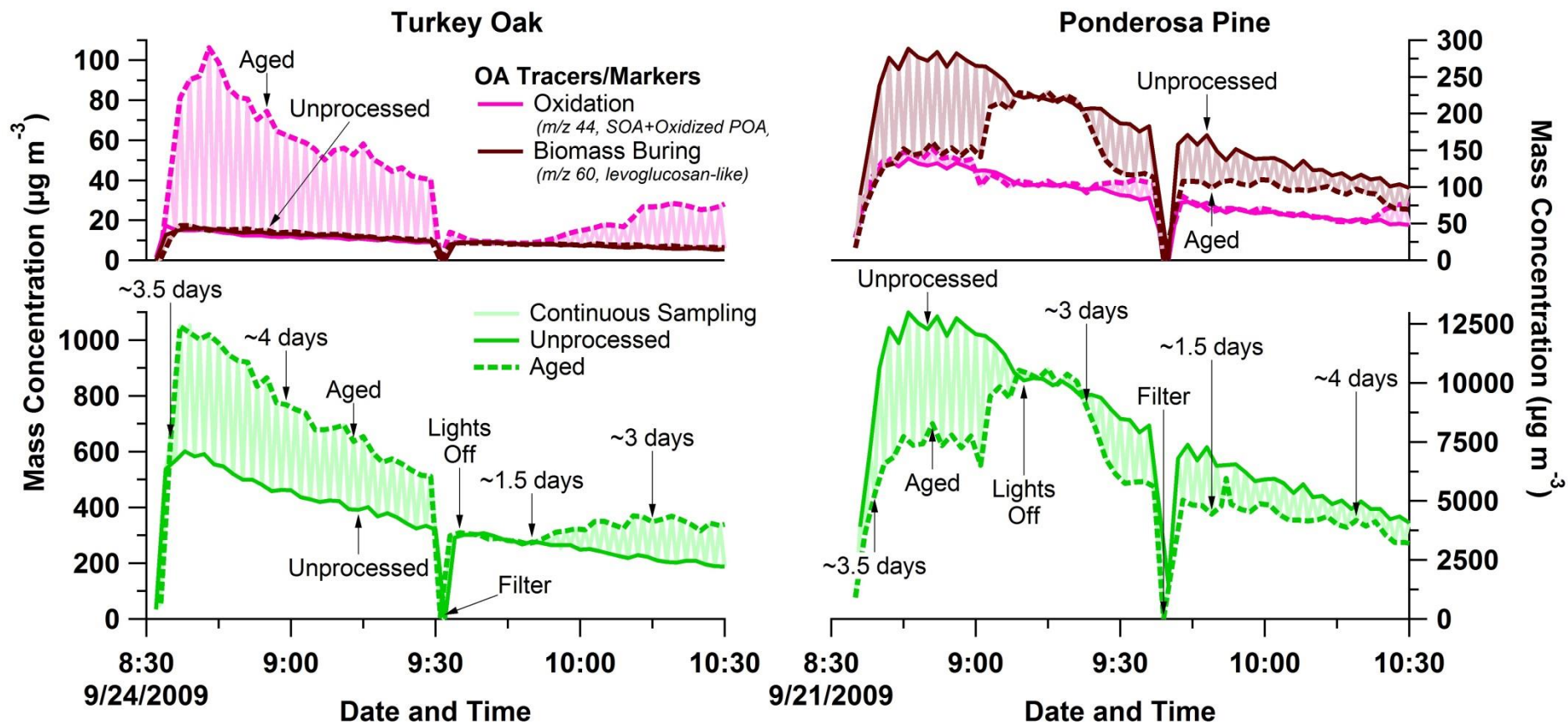


Figure S3.

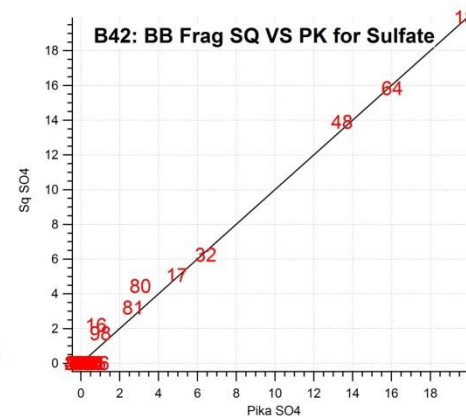
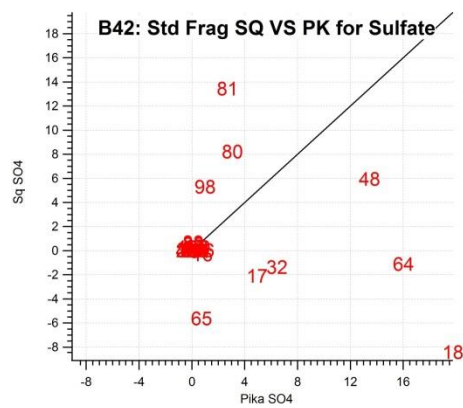
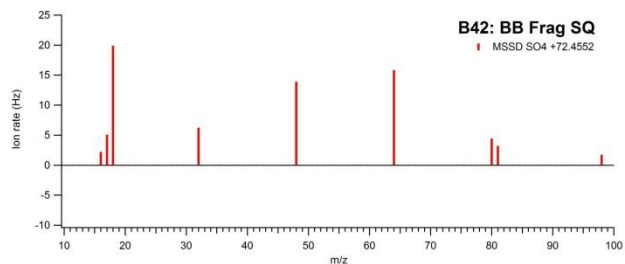
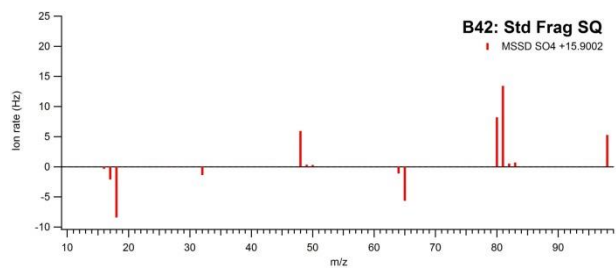
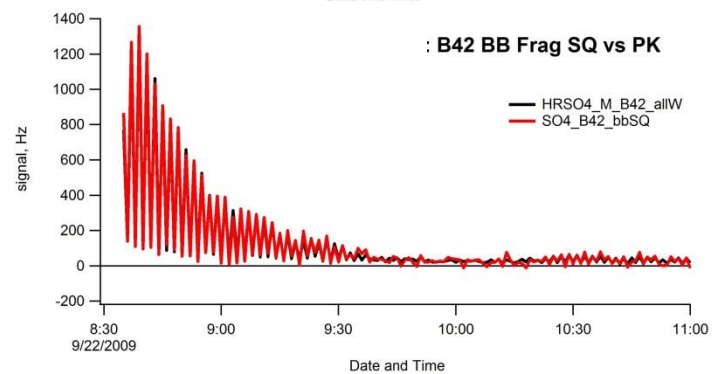
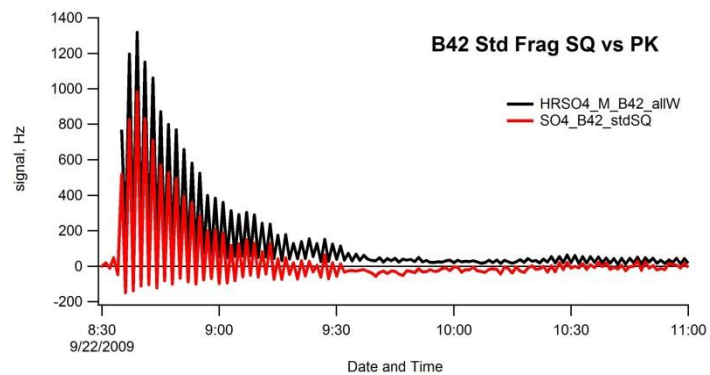
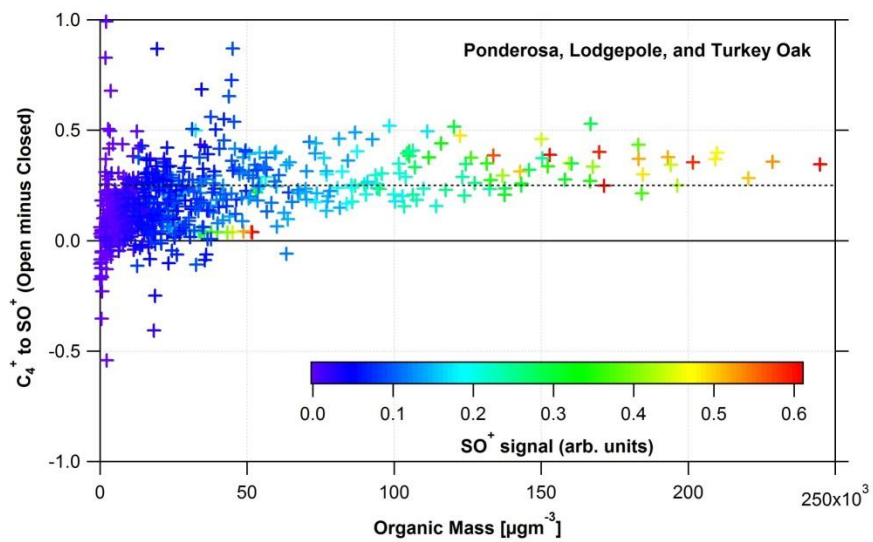


Figure S4.

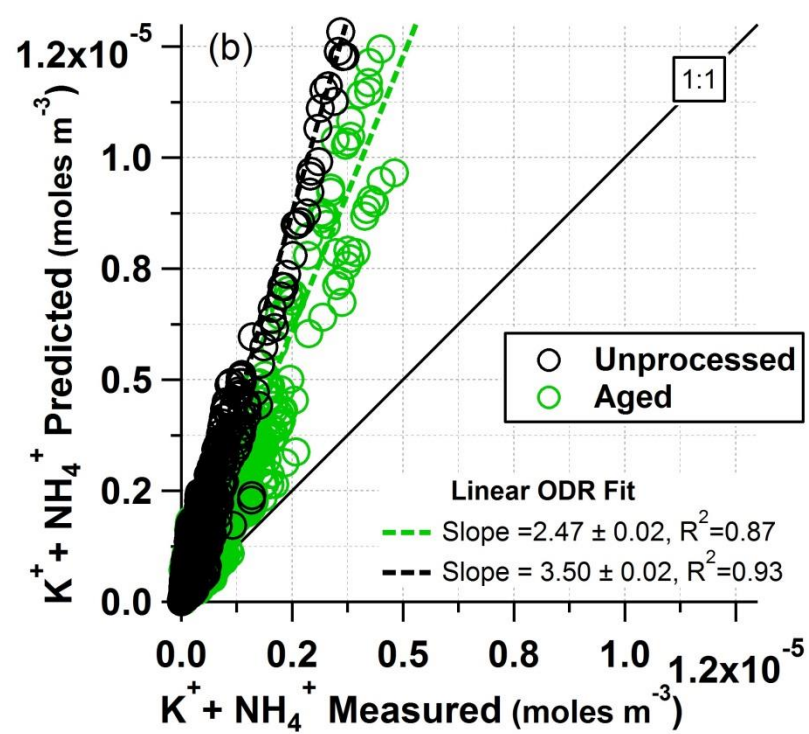
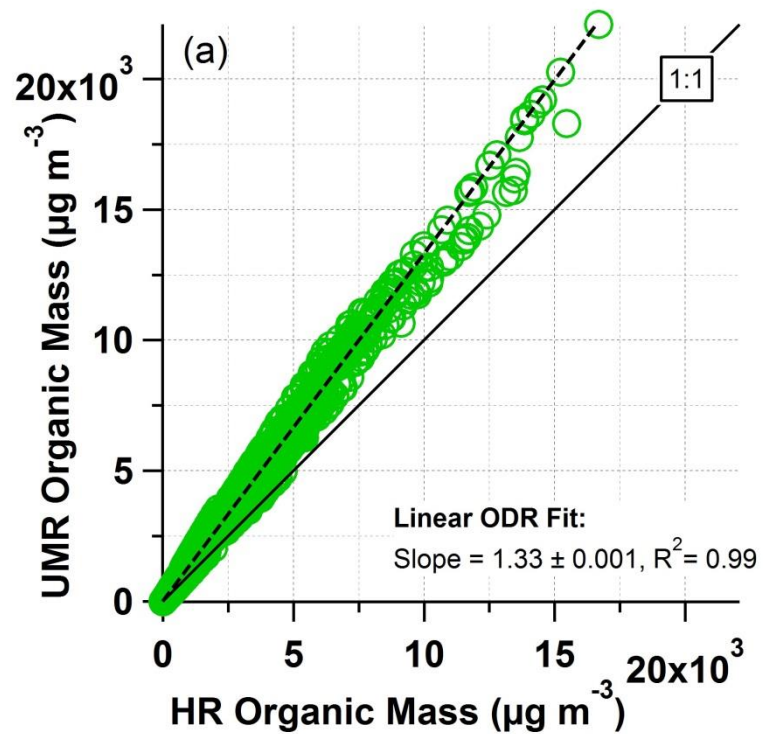


Figure S5.

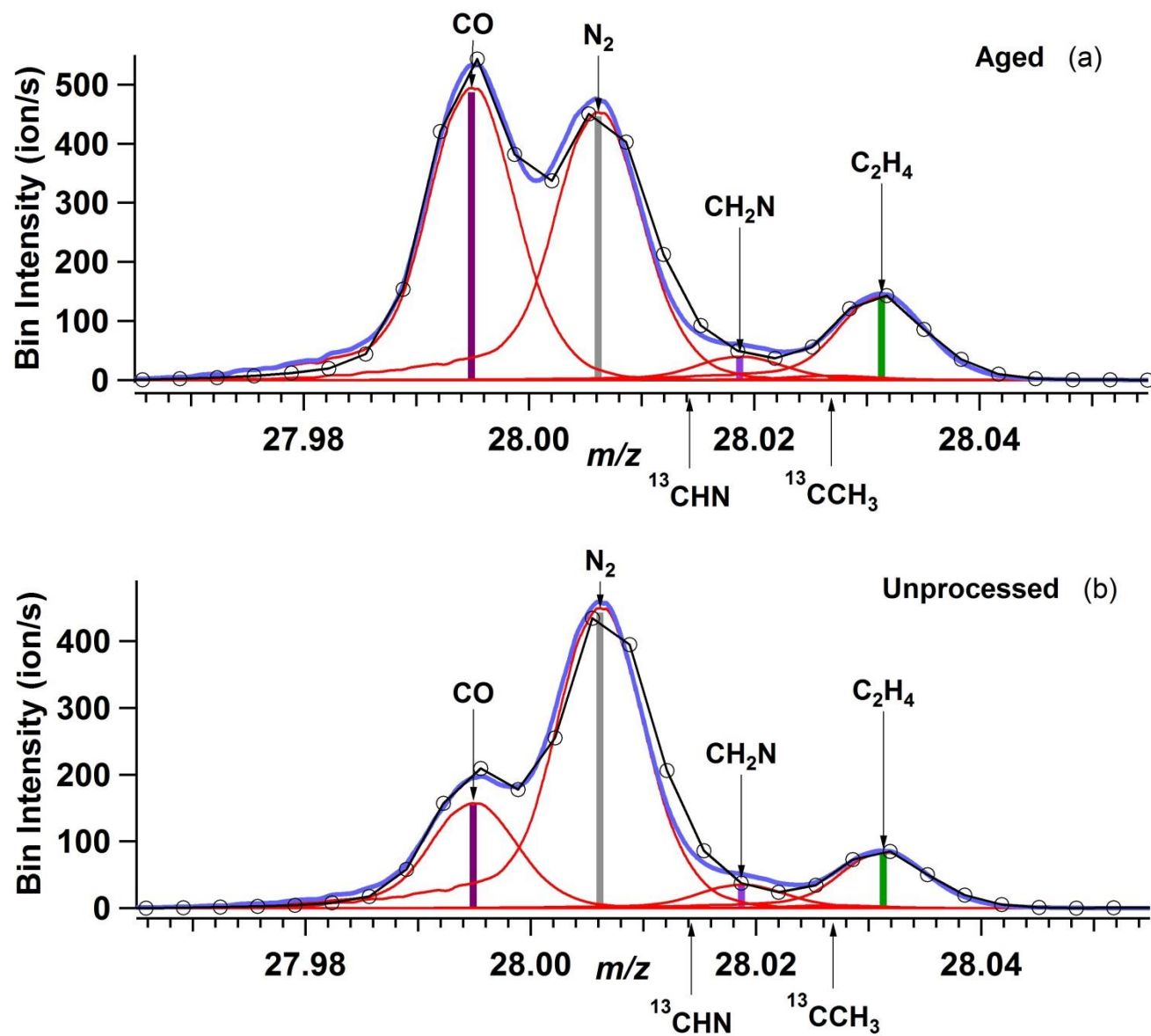


Figure S6.

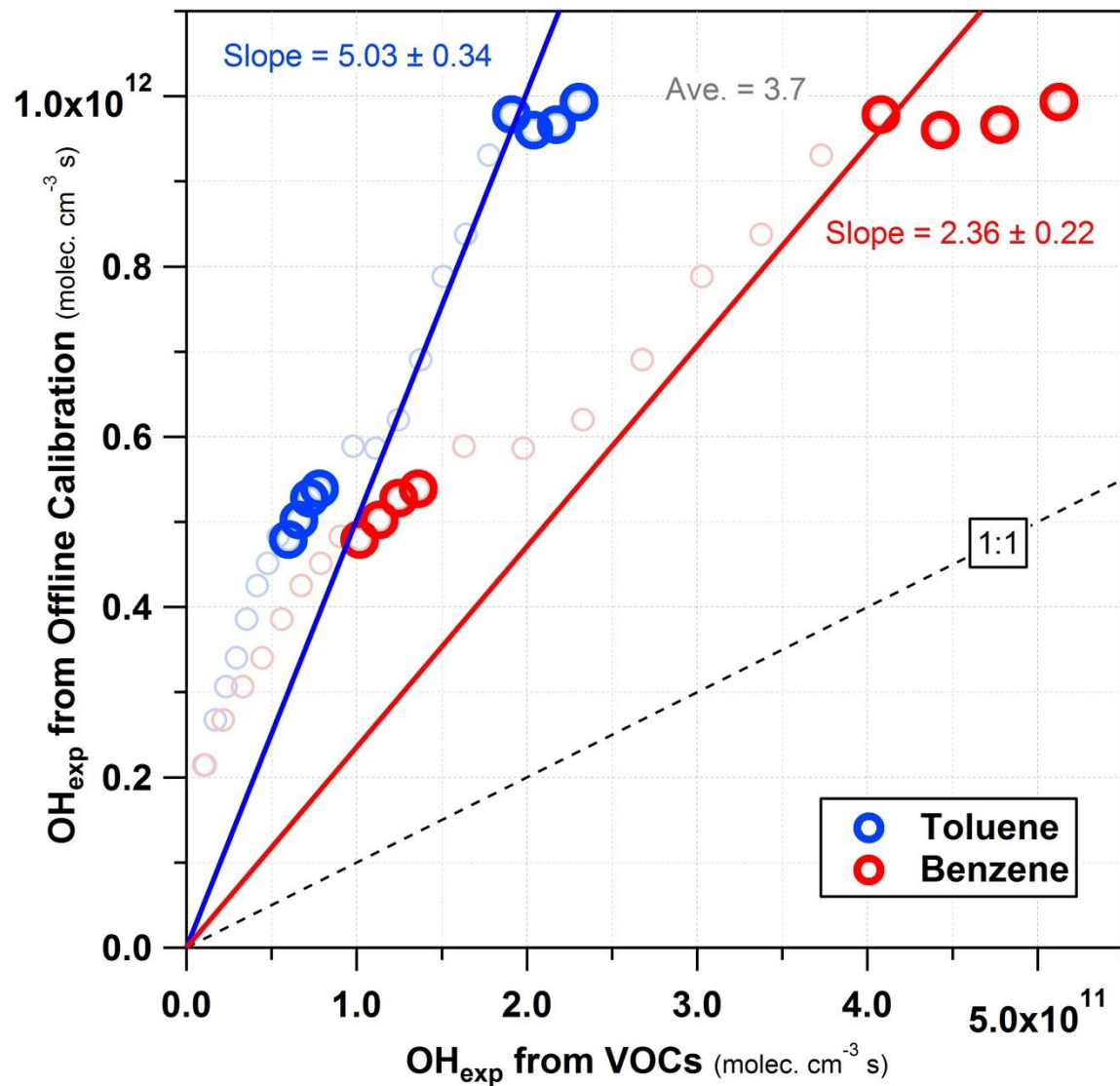


Figure S7.

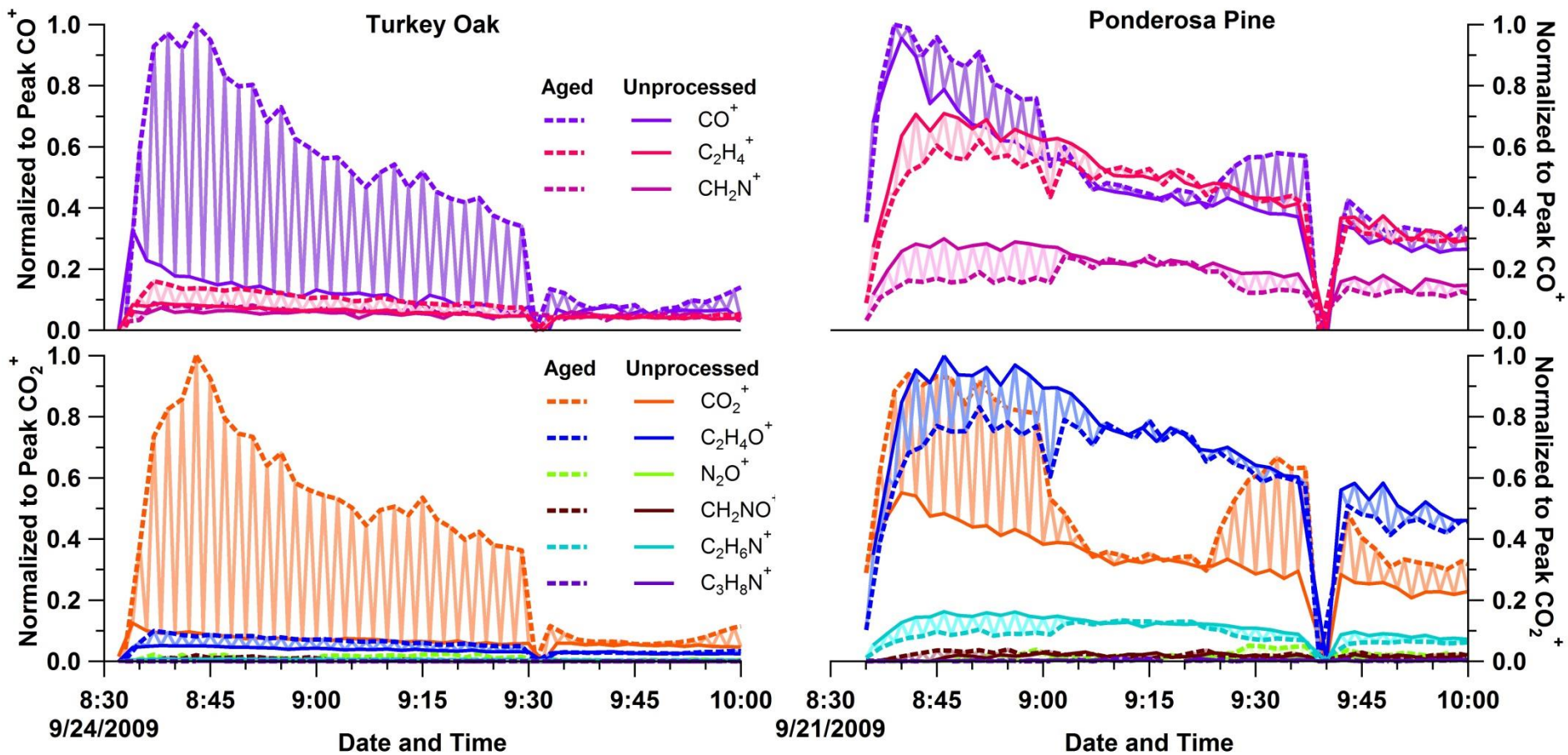


Figure S8.

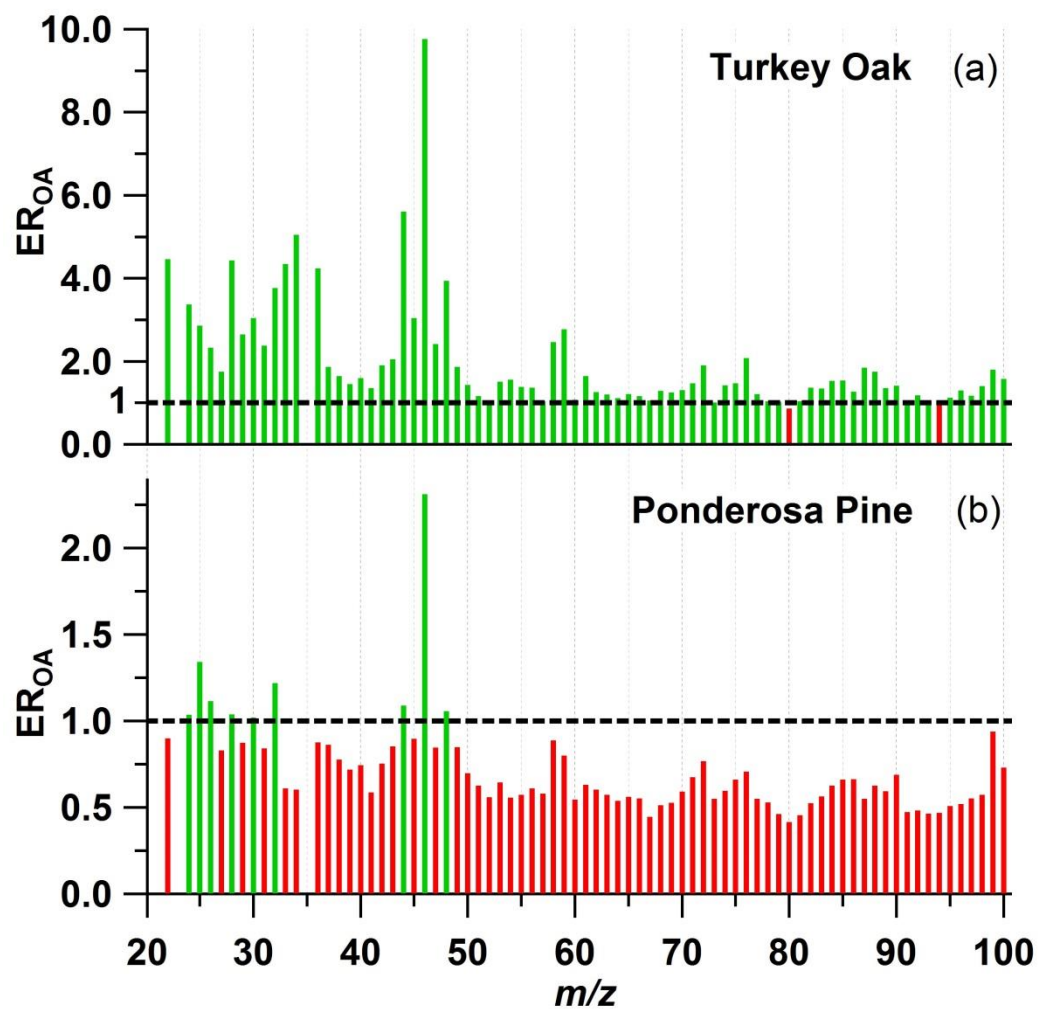


Figure S9.

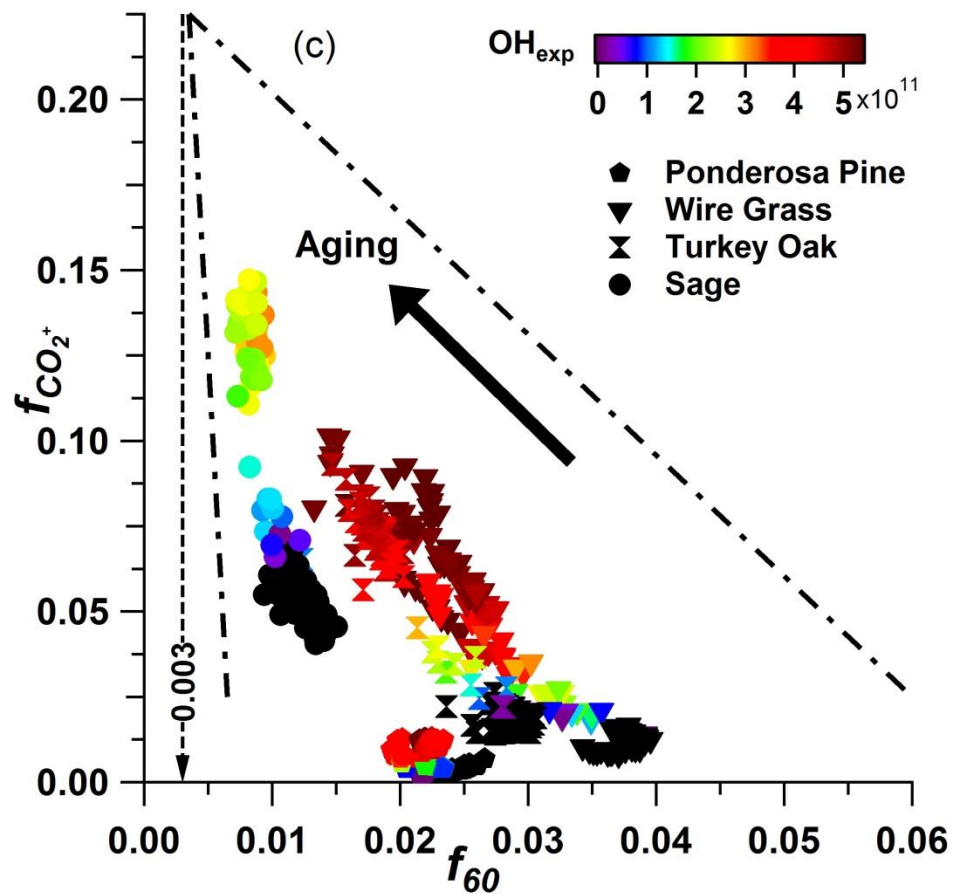
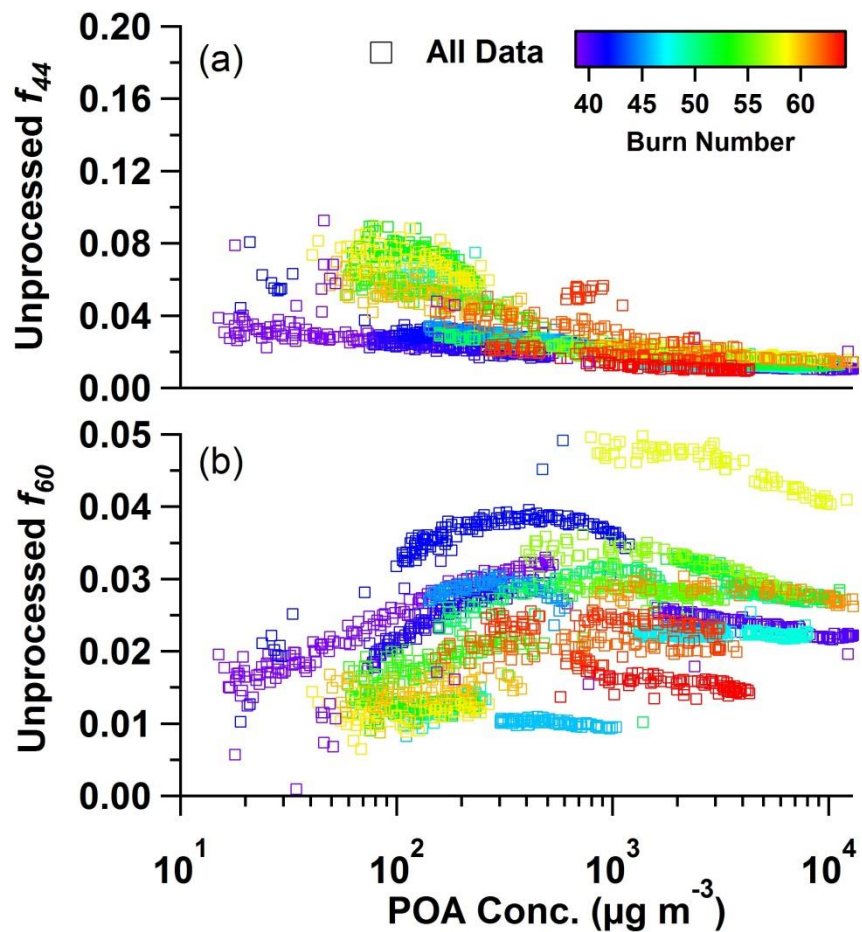


Figure S10.

